Physica B: Condensed Matter 539 (2018) 35–43

Contents lists available at ScienceDirect

Physica B: Condensed Matter

journal homepage: www.elsevier.com/locate/physb

On the half-life of luminescence signals in dosimetric applications: A unified presentation

V. Pagonis [a,*], G. Kitis [b], G.S. Polymeris [c]

[a] McDaniel College, Physics Department, Westminster, MD 21157, USA
[b] Aristotle University of Thessalonians, Physics Department, Nuclear Physics and Elementary Particles Physics Section, 54124 Thessaloniki, Greece
[c] Institute of Nuclear Sciences, Ankara University, 06100, Besevler, Ankara, Turkey

ARTICLE INFO

Keywords:
Half-life of luminescence signals
General and mixed order kinetics
OTOR model
Delocalized/localized transition model

ABSTRACT

Luminescence signals from natural and man-made materials are widely used in dosimetric and dating applications. In general, there are two types of half-lives of luminescence signals which are of importance to experimental and modeling work in this research area. The first type of half-life is the time required for the *population of the trapped charge* in a single trap to decay to half its initial value. The second type of half-life is the time required for the *luminescence intensity* to drop to half of its initial value. While there a handful of analytical expressions available in the literature for the first type of half-life, there are no corresponding analytical expressions for the second type.

In this work new analytical expressions are derived for the half-life of luminescence signals during continuous wave optical stimulation luminescence (CW-OSL) or isothermal luminescence (ITL) experiments. The analytical expressions are derived for several commonly used luminescence models which are based on *delocalized* transitions involving the conduction band: first and second order kinetics, empirical general order kinetics (GOK), mixed order kinetics (MOK) and the one-trap one-recombination center (OTOR) model. In addition, half-life expressions are derived for a different type of luminescence model, which is based on *localized* transitions in a random distribution of charges. The new half-life expressions contain two parts. The first part is inversely proportional to the thermal or optical excitation rate, and depends on the experimental conditions and on the cross section of the relevant luminescence process. The second part is characteristic of the optical and/or thermal properties of the material, as expressed by the parameters in the model.

A new simple and quick method for analyzing luminescence signals is developed, and examples are given of applying the new method to a variety of dosimetric materials. The new test allows quick determination of whether a set of experimentally measured luminescence signals originate in a single trap, or in multiple traps.

1. Introduction

Luminescence signals from natural and man made materials are widely used in dosimetric and dating applications. The most commonly used models for analyzing such signals are the general order kinetics (GOK), mixed order kinetics (MOK) and the one trap one recombination center (OTOR) model. For details of these models the reader is referred to the book by Chen and Pagonis [1]. While there are many simulation studies of luminescence phenomena within these models, there has not been much attention given to the half-life of experimentally measured luminescence signals.

In general, there are two types of half-lives of importance to modeling and experimental work in luminescence dosimetry applications. The first type of half-life is the time required for the trapped charge $n(t)$ in a single trap to decay to half its initial value; this type of half-life will be denoted by $\tau_{1/2}$ in this paper.

In experimental work one does not usually measure directly the charge loss $n(t)$ and the corresponding half-life $\tau_{1/2}$, but rather one measures the intensity $I(t)$ of the luminescence signal at time t after the start of the experiment. This luminescence intensity $I(t)$ is proportional to the derivative $-dn/dt$, with the proportionality constant depending on the experimental conditions. In practical situations experimentalists are more interested in a second type of half-life of luminescence signals,

* Corresponding author.
E-mail address: vpagonis@mcdaniel.edu (V. Pagonis).

https://doi.org/10.1016/j.physb.2018.03.054
Received 26 November 2017; Received in revised form 19 February 2018; Accepted 30 March 2018
Available online 31 March 2018
0921-4526/

which is the time required for the *luminescence intensity* $I(t)$ to drop to half of its initial value. This second type of half-life will be denoted by $T_{1/2}$ in the rest of this paper.

The purpose of this paper is to present new analytical expressions for the half-life parameters $\tau_{1/2}$ and $T_{1/2}$. The expressions are applicable for experiments carried out under either constant optical excitation, or under constant thermal excitation conditions. The new analytical expressions contain the model parameters characterizing both the experimental conditions, as well as the physical properties of the materials.

The specific goals of this work are:

1. To develop new analytical equations for both continuous-wave optically stimulated luminescence signals (CW-OSL), and for isothermal thermoluminescence (ITL) signals.
2. To investigate the effect of the various parameters in the models on the values of $\tau_{1/2}$ and $T_{1/2}$.
3. To develop a new simple test that can be applied to experimental luminescence signals, which will allow a quick determination of whether the measured luminescence signal originates in a single trap, or is due to the presence of multiple traps.

This paper is organized as follows. Sections 2 and 3 summarize previous work in this area, and develop a unified presentation of the half-life concept in the various luminescence models. Sections 4–6 present the new analytical expressions for the two half-lives $\tau_{1/2}$ and $T_{1/2}$ for models based on delocalized transitions. Section 7 presents new analytical expressions for a model based on localized transitions, and section 8 presents examples of analysis of experimental data for a variety of materials, based on a new simple test.

2. Previous analytical work on the half-life $\tau_{1/2}$ of luminescence signals

The half-life $\tau_{1/2}$ is one of fundamental parameters which can be used to characterize ITL and CW-OSL signals in radiation dosimetry and in luminescence dating. For example, in the case of a *first order* kinetics process, the charge loss $n(t)$ and the associated luminescence intensity $I(t) = -dn/dt$ are usually assumed to be an exponential function, and the half-life $\tau_{1/2}$ or $T_{1/2}$ of these processes are evaluated by the well-known first order kinetics expression:

$$\tau_{1/2} = T_{1/2} = \frac{\ln 2}{\lambda}, \tag{1}$$

where λ (s^{-1}) is the constant rate of optical or of thermal excitation. This is the only simple luminescence model in which $\tau_{1/2} = T_{1/2}$, and in which both $n(t)$ and its derivative $I(t) = -dn/dt$ are exponential functions. It is also noted that in this case the half-life is independent of the initial concentration of trapped charge ($n(0) = n_o$) at the beginning of the experiment.

Although first order kinetics is commonly assumed in the analysis of ITL/CW-OSL signals, of more general interest are the half-lives for non-first order kinetics processes. A few analytical expressions for $\tau_{1/2}$ exist in the literature, which are based on the empirical differential equation for general order kinetics, as discussed in some detail in the next section of this paper. Furetta and Kitis [3] obtained the following analytical equation for $\tau_{1/2}$ in the empirical GOK model:

$$(\tau_{1/2})_{GOK} = \frac{1}{\lambda}\left(\frac{n_0}{N}\right)^{1-b}\frac{1}{(1-b)}\left(1-\frac{1}{2^{1-b}}\right), \quad b \neq 1. \tag{2}$$

This analytical equation shows that the value of $\tau_{1/2}$ in the GOK model depends on the initial trap filling (n_o/N), and is also inversely proportional to the constant excitation rate λ. In the case of *second order* kinetics $b = 2$, Eq. (2) becomes:

$$(\tau_{1/2})_{b=2} = \frac{1}{\lambda}\frac{N}{n_0}. \tag{3}$$

Another analytical equation for $\tau_{1/2}$ has been published for the one-trap one-recombination center model (OTOR), which is the simplest and most fundamental model for luminescence simulation studies. When quasistatic equilibrium (QE) conditions are applied to the OTOR model, one obtains the General One Trap model (GOT) of luminescence phenomena [1,2]. Although various aspects of the OTOR/GOT model have been studied extensively during the past 50 years, it was only recently that analytical solutions were obtained for this model. Kitis and Vlachos [6] used the well known transcendental Lambert W function to solve the differential equation of the OTOR model. In later work Singh and Gartia [15] developed a similar equation based on the Wright Omega function. Recently Kitis and Pagonis [7] continued the work by Kitis and Vlachos [6], and presented sets of new analytical equations for several aspects of luminescence phenomena within the OTOR model. These authors obtained the following analytical equation for the half-life $\tau_{1/2}$ of charge loss $n(t)$ from a single trap, during constant optical or thermal stimulation within the OTOR model:

$$(\tau_{1/2})_{OTOR} = \frac{1}{\lambda}\left[\frac{NR}{n_0} + (1-R)\ln 2\right]. \tag{4}$$

For $R = 0$ (case of no retrapping, and first order kinetics), this equation reduces to the first order kinetics Eq. (1) in this paper, while for $R = 1$ it reduces to the second order kinetics Eq. (3). A similar equation was derived for ITL by Lovedy and Gartia [10], although their expression contains some typographical errors.

Eq. (2) and Eq. (4) give the half-life of the charge loss $n(t)$ from a trap during an ITL or during a CW-OSL process, and are derived within the GOK and OTOR models respectively.

To the best of our knowledge, there are no published corresponding analytical equations for $T_{1/2}$ in any of the luminescence models considered in this paper.

It must be clarified that the term continuous-wave optically stimulated luminescence (CW-OSL) in this paper refers to the specific experimental technique used in applications in luminescence dosimetry and luminescence dating. During the CW-OSL and IRSL experiments described here, the rate constant λ has values of the order of 0.01–1 s. The models and equations presented in this paper therefore would not apply to the stimulated emission phenomena obtained using e.g. lasers.

3. Unified presentation of the models- general analytical expressions for $\tau_{1/2}$ and $T_{1/2}$ in delocalized transition models

In this section we give a unified presentation of analytical expressions for the half-life of luminescence signals in the GOK, MOK and OTOR models. These models are based on delocalized transitions involving the conduction or valence band.

The differential equations governing the GOK, MOK, OTOR models are as follows [1]:

$$\frac{dn}{dt} = -\frac{n^b}{N^{b-1}}\lambda \qquad (GOK), \tag{5}$$

$$\frac{dn}{dt} = -\frac{n(n+M)}{M+N}\lambda \qquad (MOK) \tag{6}$$

$$\frac{dn}{dt} = -\frac{n^2}{RN+(1-R)n}\lambda \qquad (OTOR/GOT) \tag{7}$$

The symbols in these equations are as follows: n, N are the instantaneous and total concentrations of trapped electrons, b is the empirical constant for the general order kinetics, M is the total concentration of trapped electrons in a thermally disconnected trap, and R is the ratio of recombination and retrapping rates in the OTOR/GOT model. The common parameter in these models is the constant excitation rate λ (s^{-1}). For CW-OSL experiments the parameter λ represents the constant rate of optical excitation, and is given by $\lambda = \sigma P$, where σ (cm^2) is the optical cross section characterizing the optical properties of the material, and P ($photons\,s^{-1}\,cm^{-2}$) is proportional to the photon flux of the

light source. It is noted that the term CW-OSL also applies to continuous wave infrared stimulated luminescence (CW-IRSL) signals, which are common in a variety of dosimetric luminescent materials.

For ITL experiments the parameter λ represents the constant rate of *thermal* excitation, and is given by $\lambda = sexp(-E/kT)$, where E (eV) and s (s^{-1}) are the activation energy and frequency constant which characterize the thermal properties of the trap.

The previous four differential equations can be presented in a unified manner, since they can be written in the form:

$$\frac{dn}{dt} = -f(n)\lambda \tag{8}$$

where the functions $f(n)$ have the appropriate mathematical form for each model.

By rearranging the last equation and integrating from $t = 0$ to time t during the experiment, we obtain:

$$\int_0^t \lambda dt = -\int_{n_o}^{n} \frac{dn}{f(n)}. \tag{9}$$

where $n_o = n(0)$ is the initially trapped charge at time $t = 0$. In general, it may or it may not be possible to solve Eq. (9) analytically for the concentration of trapped electrons $n(t)$ as a function of the elapsed time t. However, this equation contains the relationship between n and t in parametric form, and it can be solved for the half-life $\tau_{1/2}$ as follows.

By setting $t = \tau_{1/2}$ when $n = n_o/2$ in Eq. (9), one obtains:

$$\int_0^{\tau_{1/2}} \lambda dt = -\int_{n_o}^{n_o/2} \frac{dn}{f(n)}. \tag{10}$$

For the special case $\lambda =$ constant, this gives the desired analytical expression for the half-life of the charge $n(t)$ in the single trap:

$$\tau_{1/2} = -\frac{1}{\lambda}\int_{n_o}^{n_o/2} \frac{dn}{f(n)}. \tag{11}$$

This general equation can be applied for any of the GOK, MOK and OTOR models, since it was derived by using only the assumption of $\lambda =$ constant.

We now proceed to derive the general analytical equation for the second type of half-life $T_{1/2}$, which can be measured directly and quickly in experimental work.

The intensity $I(t)$ is given by the negative derivative of the charge loss $n(t)$:

$$I(t) = -\frac{dn}{dt} = f(n)\lambda \tag{12}$$

At time $t = 0$ the initial intensity $I_o = I(0)$ is found by setting $n = n_o$:

$$I_o = f(n_o)\lambda \tag{13}$$

Let us denote by $n = n_{1/2}$ the charge remaining in the trap when the luminescence intensity has dropped to half its initial value, i.e. $n = n_{1/2}$ when $I = I_o/2$. Substituting $n = n_{1/2}$ and $I = I_o/2$ in Eq. (12) we obtain:

$$\frac{I_o}{2} = f(n_{1/2})\lambda \tag{14}$$

Substituting the value of I_o from Eq. (13) into Eq. (14):

$$\frac{f(n_o)}{2} = f(n_{1/2}) \tag{15}$$

This is a general equation which can be used to find the concentration $n_{1/2}$, and its solution can be either obtained analytically as in some of the examples in this paper, or it can be evaluated by numerically solving for $n_{1/2}$. Now by setting $t = T_{1/2}$ when $n = n_{1/2}$ in Eq. (9), one obtains:

$$\int_0^{T_{1/2}} \lambda dt = -\int_{n_o}^{n_{1/2}} \frac{dn}{f(n)}. \tag{16}$$

For the special case $\lambda =$ constant, this gives the desired analytical expression for the half-life $T_{1/2}$ of the luminescence intensity $I(t)$:

$$T_{1/2} = -\frac{1}{\lambda}\int_{n_o}^{n_{1/2}} \frac{dn}{f(n)}. \tag{17}$$

This is again a general equation which can be applied for any of the analytical models, and it also applies to either ITL or CW-OSL experiments.

In the next five sections we apply the general Eq. (11) and Eq. (17) to the GOK, MOK, OTOR/GOT delocalized transition models.

4. Analytical expressions for $\tau_{1/2}$ and $T_{1/2}$ in the GOK model

Furetta and Kitis [3] obtained previously the analytical Eq. (2) for $\tau_{1/2}$ in the empirical GOK model. In this section we derive the corresponding GOK expression for $T_{1/2}$.

Substituting $f(n) = \frac{n^b}{N^{b-1}}$ from Eq. (5) into the general Eq. (17):

$$T_{1/2} = -\frac{1}{\lambda}\int_{n_o}^{n_{1/2}} \frac{dn}{f(n)} = -\frac{1}{\lambda(b-1)} N^{b-1}\left(n_o n_{1/2}\right)^{-b}\left[\left(n_{1/2}\right)^b n_o - n_{1/2}(n_o)^b\right] \tag{18}$$

Similarly substituting $f(n) = \frac{n^b}{N^{b-1}}$ in the general Eq. (15):

$$\frac{1}{2}\frac{n_o^b}{N^{b-1}} = \frac{n_{1/2}^b}{N^{b-1}} \tag{19}$$

or

$$n_{1/2} = \frac{1}{2^{1/b}} n_o \tag{20}$$

By substituting this value of $n_{1/2}$ into Eq. (18) and simplifying, one obtains:

$$\left(T_{1/2}\right)_{GOK} = \frac{(N/n_0)^{b-1}}{\lambda(b-1)}\left[-1 + 2^{\frac{b-1}{b}}\right] \tag{21}$$

This analytical equation shows that the value of $T_{1/2}$ in the GOK model depends on the initial trap filling (n_o/N), and is also inversely proportional to the excitation constant λ. For $b \to 1$ the limit of this function is found by using L'Hospital's rule, and is the expected first order kinetics expression $T_{1/2} = \frac{\ln 2}{\lambda}$, while for $b \to 2$ this equation gives $T_{1/2} = (N/n_o)\left(-1 + \sqrt{2}\right)/\lambda$.

Fig. 1(a) shows a plot of the dimensionless quantities $\lambda\tau_{1/2}$ and $\lambda T_{1/2}$ in the GOK model, as a function of the general order kinetic parameter b, and for two values of the initial trap filling ratio $n_o/N = 0.01$, 0.5. The curves in Fig. 1(a) show that for $b = 1$ the half-lives $\tau_{1/2}$ and $T_{1/2}$ do not depend on the initial trap filling ratio n_o/N. By contrast, in the limit of $b = 2$ these curves show clearly that there is a dependence of these half-lives on the ratio n_o/N.

5. Analytical equations for $\tau_{1/2}$ and $T_{1/2}$ in the MOK model

In this section we apply the general equations in the case of the MOK model, which can be considered as a "mixture" of first and second order kinetics. For the MOK model the function $f(n) = \frac{n(n+M)}{N+M}$, and the general Eq. (11) becomes:

$$\tau_{1/2} = -\frac{1}{\lambda}(N+M)\int_{n_o}^{n_o/2} \frac{dn}{n(n+M)}. \tag{22}$$

By integrating and by following essentially the same method as in the previous section, we find the half-life $\tau_{1/2}$:

$$\tau_{1/2} = \frac{1}{\lambda}\frac{N+M}{M}\ln\left[\frac{2M+n_o}{n_o+M}\right] \tag{23}$$

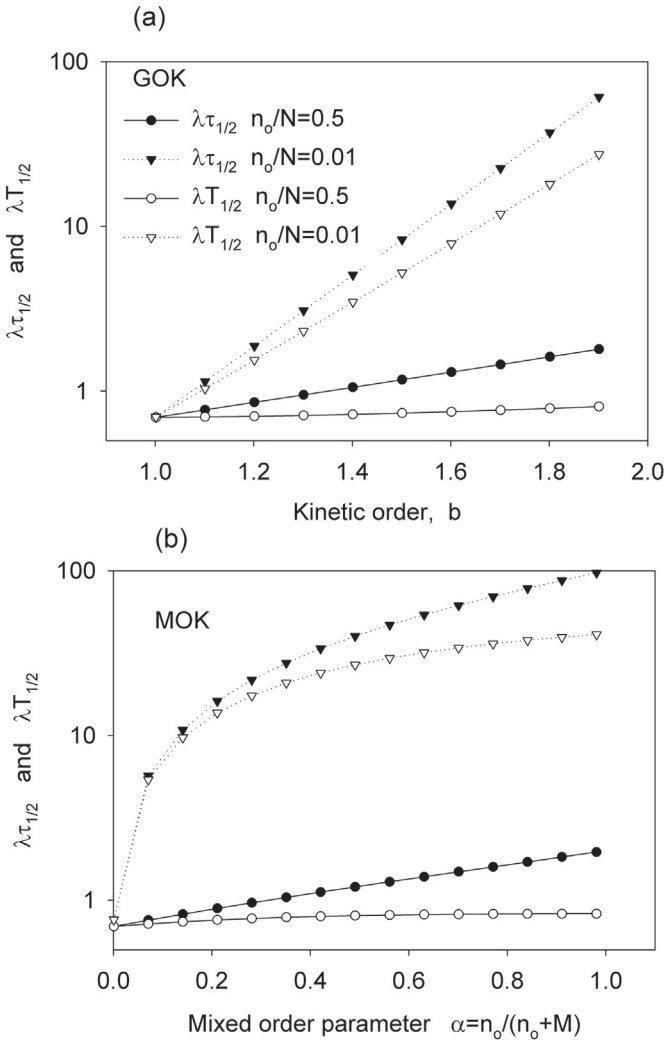

Fig. 1. (a) A plot of $\lambda\tau_{1/2}$ and $\lambda T_{1/2}$ in the GOK model as a function of the kinetic order parameter b, and for two values of the initial trap filling ratio $n_o/N = 0.01, 0.5$ (b) The same plot for the MOK model, as a function of the mixed order parameter α.

Instead of the parameter M, it is customary to define the following dimensionless parameter α to characterize mixed order kinetics [1].

$$\alpha = \frac{n_o}{n_o + M} \tag{24}$$

One expects that the MOK model in the limit $\alpha \to 0$ will give first order kinetics, while in the limit $\alpha \to 1$ the MOK model should give second order kinetics.

By substituting Eq. (24) into Eq. (23):

$$(\tau_{1/2})_{MOK} = \frac{1}{\lambda}\left(1 + \frac{N\alpha}{n_o(1-\alpha)}\right)\ln[2-\alpha] \tag{25}$$

For $\alpha \to 0$ the limit of this function is the expected first order kinetics expression $\tau_{1/2} \to \ln 2/\lambda$, while for $\alpha \to 1$ the application of L'Hospital's rule gives the second order kinetics expression $\tau_{1/2} = (N/n_o)/\lambda$.

Similarly, in order to calculate the half-life $T_{1/2}$, we substitute $f(n) = \frac{n(n+M)}{N+M}$ in the general Eq. (15):

$$\frac{1}{2}n_o(n_o + M) = n_{1/2}(n_{1/2} + M) \tag{26}$$

This is a quadratic equation for the parameter $n_{1/2}$ and its positive root solution is:

$$(n_{1/2})_{MOK} = \frac{1}{2}\left(-M + \sqrt{M^2 + 2Mn_o + 2n_o^2}\right) \tag{27}$$

Finally by substituting this value of $n_{1/2}$ into Eq. (17) and simplifying, we obtain:

$$(T_{1/2})_{MOK} = \frac{1}{\lambda}\left(1 + \frac{N\alpha}{n_o(1-\alpha)}\right)\ln\left[1 - \alpha + \alpha^2 + (1-\alpha)\sqrt{1+\alpha^2}\right] \tag{28}$$

For $\alpha \to 0$ the limit of this function is the expected first order kinetics expression $T_{1/2} = \ln 2/\lambda$, while for $\alpha \to 1$ this gives the second order expression $T_{1/2} = (N/n_o)\left(-1 + \sqrt{2}\right)/\lambda$.

Both analytical expressions for $\tau_{1/2}$ and for $T_{1/2}$ in the MOK model are proportional to $\frac{1}{\lambda}$, and they also depend on the mixed order parameter α, and on the initial trap filling ratio (n_o/N).

A plot of $\lambda\tau_{1/2}$ and for $\lambda T_{1/2}$ in the MOK model as a function of the mixed order parameter α is shown in Fig. 1(b), and for two values of the initial trap filling ratio $n_o/N = 0.01, 0.5$. The qualitative behavior of the MOK model in Fig. 1(b), is similar to the behavior of the GOK model in Fig. 1(a). This is not surprising, since both models attempt to describe mathematically the kinetic behavior of a process in-between first and second order kinetics.

6. Analytical expressions for $\tau_{1/2}$ and $T_{1/2}$ in the OTOR/GOT model

In this section we apply the general equations in the case of the OTOR model. Due to the complexity of the algebra involved, the commercial software package *Mathematica* was used to test the algebraic calculations in this and in the next section.

For the OTOR/GOT model the function $f(n) = \frac{n^2\lambda}{RN+(1-R)n}$ and the general Eq. (11) becomes:

$$\tau_{1/2} = -\frac{1}{\lambda}\int_{n_o}^{n_o/2}\frac{RN + (1-R)n}{n^2}\,dn. \tag{29}$$

This can be integrated and simplified to yield the following expression:

$$(\tau_{1/2})_{OTOR} = \frac{1}{\lambda}\left[\frac{NR}{n_0} + (1-R)\ln 2\right]. \tag{30}$$

As expected, this equation is identical to Eq. (4) in this paper, derived in the recent work by Kitis and Pagonis [7].

Similarly by substituting $f(n) = \frac{n^2\lambda}{RN+(1-R)n}$ in the general Eq. (15):

$$\frac{1}{2}\frac{n_o^2\lambda}{RN + (1-R)n_o} = \frac{n_{1/2}^2\lambda}{RN + (1-R)n_{1/2}} \tag{31}$$

This is a quadratic equation for the value $n_{1/2}$, and its positive root solution is:

$$(n_{1/2})_{OTOR} = \frac{n_o}{4}\frac{\gamma(R-1) + \sqrt{\gamma^2(R-1)^2 - 8R\gamma(R-1) + 8R^2}}{R - \gamma(R-1)} \tag{32}$$

where $\gamma = n_o/N$ is the degree of initial filling of the traps.

Finally substituting Eq. (32) into Eq. (17), we obtain:

$$T_{1/2} = -\frac{1}{\lambda}\int_{n_o}^{n_{1/2}}\frac{RN + (1-R)n}{n^2}\frac{dn}{f(n)} \tag{33}$$

which yields:

$$(T_{1/2})_{OTOR} = \frac{1}{2\lambda}\left(-1 - 2R/\gamma + R + A - 2\ln\frac{A - R + 1}{4(1 + R/\gamma - R)} - 2R\ln\frac{A + R - 1}{2R/\gamma}\right) \tag{34}$$

where the dimensionless parameter A is defined as:

$$A = \sqrt{(R-1)^2 - 8R(R-1)/\gamma + 8R^2/\gamma^2} \tag{35}$$

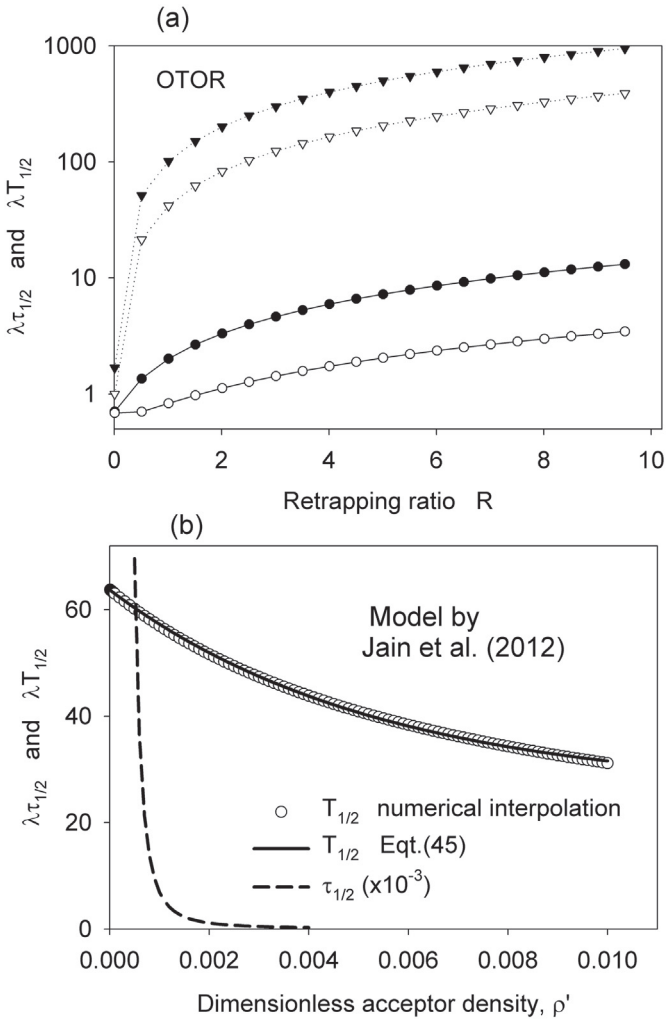

Fig. 2. (a) A plot of $\lambda\tau_{1/2}$ (black symbols) and $\lambda T_{1/2}$ (white symbols) in the OTOR/GOT model as a function of the retrapping ratio R, and for two values of the initial trap filling ratio $n_o/N = 0.01$, 0.5 (triangles and circles correspondingly) (b) A plot of $\lambda\tau_{1/2}$ and $\lambda T_{1/2}$ in the localized transition model of [5], as a function of the dimensionless acceptor density parameter ρ'.

This is the desired analytical expression for $T_{1/2}$ in the OTOR model, in terms of the parameters λ, R, γ. For $R \to 0$ the limit of this function is the first order expression $T_{1/2} \to \ln 2/\lambda$, while for $R \to 1$ this gives the second order expression $T_{1/2} = (N/n_o)\left(-1+\sqrt{2}\right)/\lambda$.

Eq. (34) for $(T_{1/2})_{OTOR}$ in the OTOR model was tested for random values of the parameters in the range $R = 10^{-4}$–10 and $\gamma = n_o/N = 0.01$–0.99. In all cases examined, this expression for $T_{1/2}$ was found to be accurate within better than 1%.

Once more, it is noted that both analytical expressions for $\tau_{1/2}$ and for $T_{1/2}$ in the OTOR model are proportional to $\frac{1}{\lambda}$.

Fig. 2(a) shows a plot of $\lambda\tau_{1/2}$ (black symbols) and $\lambda T_{1/2}$ (white symbols) in the OTOR model, as a function of the retrapping parameter R, and for two values of the initial trap filling ratio $n_o/N = 0.01$, 0.5 (triangles and circles correspondingly).

7. Derivation of $\tau_{1/2}$ and $T_{1/2}$ in the random charge distribution model by Jain et al. [5]

In this section we derive an analytical equation for $\tau_{1/2}$ and $T_{1/2}$ in the localized transition model of Jain et al. [5]. Kitis and Pagonis [8] showed that the loss of charge $n(t)$ in this model is described by the equation:

$$n(t) = n_o \exp\left[-\rho'\{\ln(1+z\lambda t)\}^3\right] \tag{36}$$

where ρ' represents the constant number density of acceptors, and $z = 1.8$ is a constant in the model. In this equation the time appears in the dimensionless parameter λt, so we expect that the half-lives $\tau_{1/2}$ and $T_{1/2}$ will again scale as $1/\lambda$, as in the delocalized models studied in the previous sections.

By setting $n(t) = n_o/2$ and $t = \tau_{1/2}$ in this equation, we find after some simple algebra that the half-life $\tau_{1/2}$ characterizing the decay of charge is given by the analytical equation:

$$\tau_{1/2} = \frac{1}{\lambda z}\left\{\exp\left[\left(\frac{\ln 2}{\rho'}\right)^{1/3}\right] - 1\right\} \tag{37}$$

For this model it is not possible to obtain a simple analytical expression for the lifetime $T_{1/2}$. However, it is possible to obtain numerically the values of $T_{1/2}$ for any values of the parameter ρ' in the model by using the following procedure.

For a random value of the parameter ρ' in the experimental range $\rho' = 10^{-2}$–10^{-6}, the derivative dn/dt is evaluated from the analytical Eq. (36):

$$dn/dt = -3n_o\rho' z\lambda \frac{\{\ln(1+z\lambda t)\}^2}{(1+z\lambda t)} \exp\left[-\rho'\{\ln(1+z\lambda t)\}^3\right] \tag{38}$$

By using this analytical expression, numerical interpolation is used to obtain the value of time $t = T_{1/2}$ at which the initial value of the derivative dn/dt drops to half its value.

The results of this evaluation are shown in Fig. 2(b), which shows the dimensionless quantities $\lambda\tau_{1/2}$ and $\lambda T_{1/2}$ as a function of the acceptor density ρ'. The results for $T_{1/2}$ can be fitted very accurately with the following empirical equation for the entire range of values $\rho' = 10^{-2}$–10^{-6}:

$$T_{1/2} = \frac{1}{\lambda}\left[25.65 + 38.08\exp(-185.8\rho')\right] \tag{39}$$

which gives the inverse empirical relationship:

$$\rho' = -0.00538\ln[0.0263(-25.65 + \lambda T_{1/2})] \tag{40}$$

8. A simple experimental test for the presence of multiple components in the luminescence signal

All analytical expressions derived in the present work are summarized in Table 1, and they are all found to be inversely proportional to the constant excitation rate λ. By taking the natural logarithm of the general Eq. (17), we obtain:

$$\ln(T_{1/2}) = -\ln(\lambda) + \ln\left(\int_{n_{1/2}}^{n_o} \frac{dn}{f(n)}\right) = -\ln(\lambda) + \ln(\text{constant}).$$

This equation suggests that within the context of these models and for signals originating from a single trap, a plot of $\ln(T_{1/2})$ vs. $\ln(\lambda)$ should be a straight line with a slope of −1. Any large deviation of this plot from a straight line, or a large deviation from a slope of −1, could then be interpreted as due to the presence of multiple competing traps contributing to the same luminescence signal, or as indicating the possible presence of strong competition effects during the CW-OSL and CW-IRSL measurements.

On the basis of this observation, the following simple experimental test is suggested for *CW-OSL* or *CW-IRSL data*:

- Measure the CW-OSL or CW-IRSL luminescence signals for different constant stimulating powers of the exciting source.
- From the experimental luminescence intensity vs time curves $I(t)$, find the times $T_{1/2}$ required for the intensity to drop to half its initial value.

Table 1
Summary of analytical equations derived in this work for first and second order kinetics, GOK, MOK and OTOR models.

Equation for $\tau_{1/2}$	Equation for $T_{1/2}$
First Order Kinetics $(\tau_{1/2})_{b=1} = \frac{\ln 2}{\lambda}$	$(T_{1/2})_{b=1} = \frac{\ln 2}{\lambda}$
Second Order Kinetics $(\tau_{1/2})_{b=2} = (N/n_o)/\lambda$	$(T_{1/2})_{b=2} = (N/n_o)\left(-1+\sqrt{2}\right)/\lambda$
General Order Kinetics $(\tau_{1/2})_{GOK} = \frac{1}{\lambda}\left(\frac{n_0}{N}\right)^{1-b}\frac{1}{(1-b)}(1-\frac{1}{2^{1-b}}),\ b \neq 1\,.$	$(T_{1/2})_{GOK} = \frac{(N/n_0)^{b-1}}{\lambda(b-1)}\left[-1+2^{\frac{b-1}{b}}\right],\ b \neq 1\,.$
Mixed Order Kinetics $(\tau_{1/2})_{MOK} = \frac{1}{\lambda}\left(1+\frac{N\alpha}{n_0(1-\alpha)}\right)\ln[2-\alpha]$	$(T_{1/2})_{MOK} = \frac{1}{\lambda}\left(1+\frac{N\alpha}{n_0(1-\alpha)}\right)\ln\left[1-\alpha+\alpha^2+(1-\alpha)\sqrt{1+\alpha^2}\right]$
OTOR/GOT $(\tau_{1/2})_{OTOR} = \frac{1}{\lambda}\left(\frac{NR}{n_0}+(1-R)\ln 2\right).$	$(T_{1/2})_{OTOR} = \frac{1}{2\lambda}\left(-1-2R/\gamma+R+A-2\ln\frac{A-R+1}{4(1+R/\gamma-R)}-2R\ln\frac{A+R-1}{2R/\gamma}\right)$ with $A = \sqrt{(R-1)^2-8R(R-1)/\gamma+8R^2/\gamma^2}$
Jain et al. [5] $(\tau_{1/2})_{Jain\ et\ al} = \frac{1}{\lambda z}\left\{\exp\left[\left(\frac{\ln 2}{\rho'}\right)^{1/3}\right]-1\right\}$	$(T_{1/2})_{Jain\ et\ al} = \frac{1}{\lambda}\left[25.65+38.08\exp(-185.8\rho')\right]$

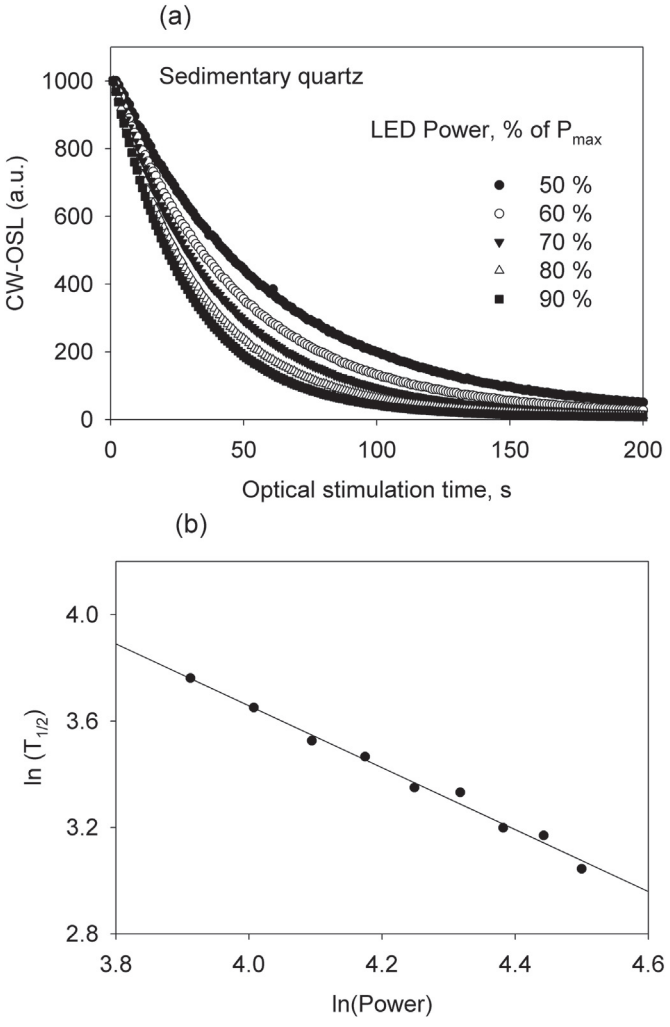

Fig. 3. (a) CW-OSL signals from a sedimentary quartz sample, measured with a variable stimulating power *P* (b) Half-lives of the data in (a) as a function of the stimulating power *P*, plotted on log-log scale.

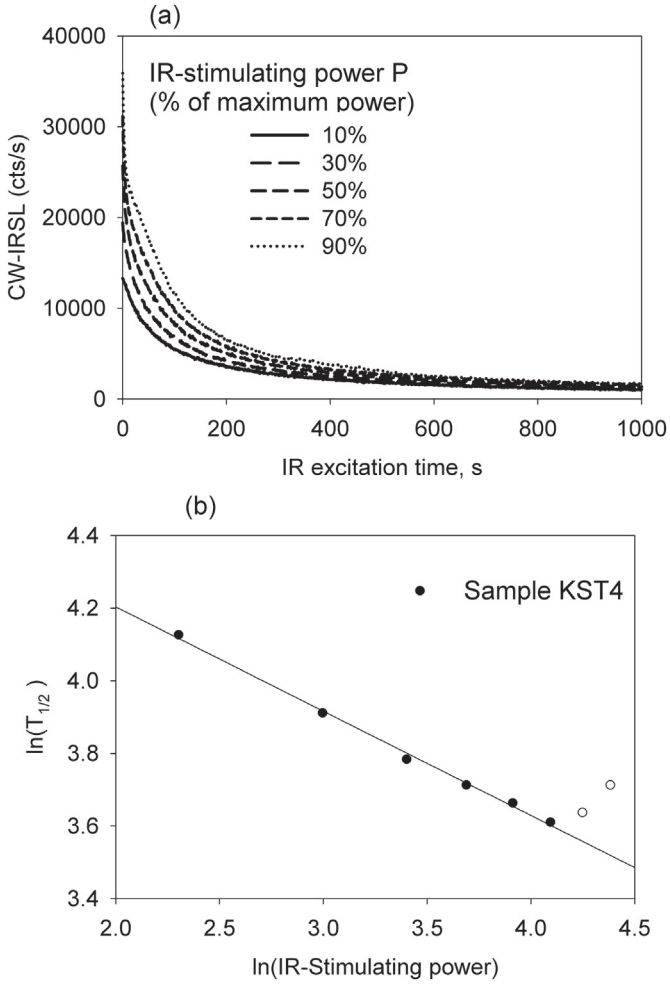

Fig. 4. (a) CW-IRSL signals from a microcline (b) A log-log plot of the half-lives of the curves in (a), as a function of the stimulating IR power.

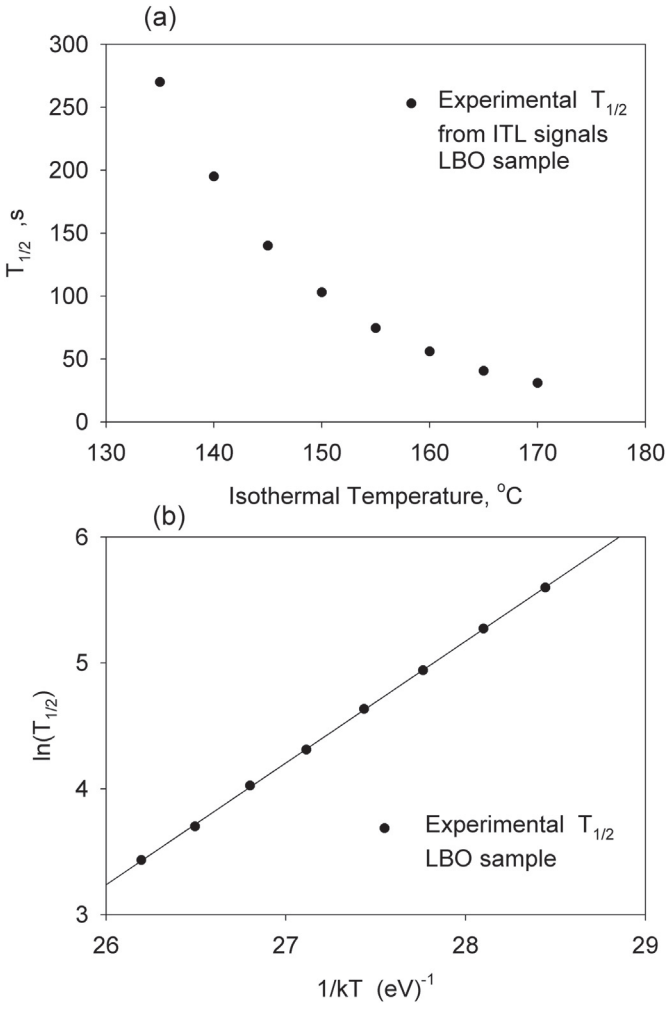

Fig. 5. (a) Half-lives of isothermal signals from sample LBO from Kitis et al. [9], measured at different temperatures in the range 135–170 °C (b) An Arrhenius plot of the data in (a) yields the activation energy E.

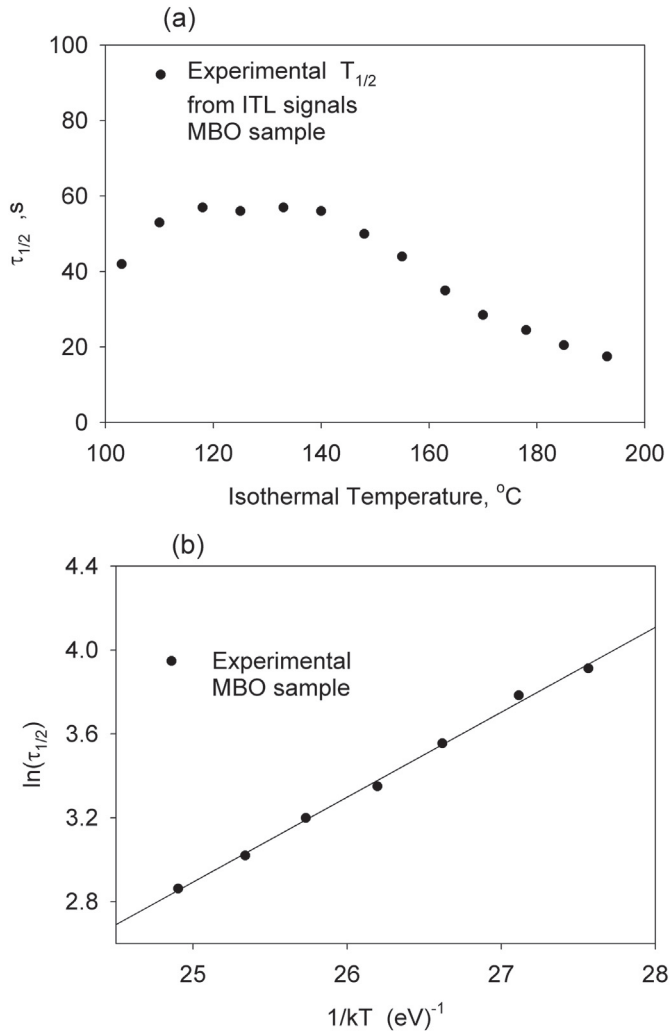

Fig. 6. (a) Half-lives of isothermal signals from sample MBO from Kitis et al. [9], measured at different temperatures in the range 100–195 °C (b) An Arrhenius plot of the same data in the temperature subrange 140–195 °C yields the activation energy E.

- Plot the logarithm of the half-life values $\ln(T_{1/2})$ as a function of the logarithm of the stimulating power $\ln(\lambda)$. If a straight line with a slope close to -1 is obtained in this plot, this is a strong indication that these signals may be originating from a single trap. A deviation from a straight line and/or a large deviation from a slope of -1, may be caused by the presence of multiple traps contributing to the luminescence signals, although other possibilities like competition effects are also a possible explanation.

For isothermal luminescence experiments (ITL) the thermal excitation rate is $\lambda = sexp(-E/k_BT)$ and the experimental test can be carried out as follows:

- Measure the ITL luminescence signals for different temperatures T.
- From the experimental ITL intensity vs time curves $I(t)$, find the times $T_{1/2}$ required for the ITL signal to drop to half its initial value.
- Plot the logarithm of the half-life values $\ln(T_{1/2})$ as a function of the Arrhenius factor $1/k_BT$. If a straight line is obtained in this plot, this is a strong indication that these signals originate from a single trap, and the slope of this line represents the thermal activation energy E of the corresponding luminescence process. A deviation from a straight line may again indicate the presence of a more complex luminescence process.

A first example of applying the simple test to CW-OSL signals from quartz is shown in Fig. 3. The sample was a milky sedimentary unheated quartz sample from Northern Greece, and the experimental data in this figure are obtained directly from the detailed study by Polymeris [14]. The CW-OSL decay curves were measured at the same temperature of 35 °C for different optical stimulation intensities, expressed as percentages of the maximum power for the blue LEDs (470 nm, FWHM 20 nm) delivering a maximum of (20 mW/cm^2) at the sample position. The power level was software controlled in the RISØ TL/OSL reader (model TL/OSL–DA–15). The detection optics consisted of a 7.5 mm Hoya U-340 filter (average λ = 340 nm, FWHM 80 nm).

The experimental CW-OSL data is shown in Fig. 3(a), as a function of the variable stimulating power P. The results of applying the test to the data in (a) is shown in Fig. 3(b), which results in a straight line with a slope of -1.16 ± 0.05 and a coefficient of $R^2 = 0.989$. This is a strong indication that the CW-OSL signals are likely to originate from the same single trap.

A second example of applying our simple test to CW-IRSL signals from a microcline sample (laboratory code KST4) is shown in Fig. 4. This sample was studied previously in Polymeris et al. [13], and Pagonis et al. [12], by using an IRSL stimulation wavelength of 875 (±40) nm and a maximum power of 135 mW/cm^2. The CW-IRSL curves from this sample measured with a variable stimulating power P are shown in Fig. 4(a), and the results of applying the test to this data is shown in Fig. 4(b). The two experimental points for higher stimulating powers of 70% and 80% deviate from the straight line fit. This behavior indi-

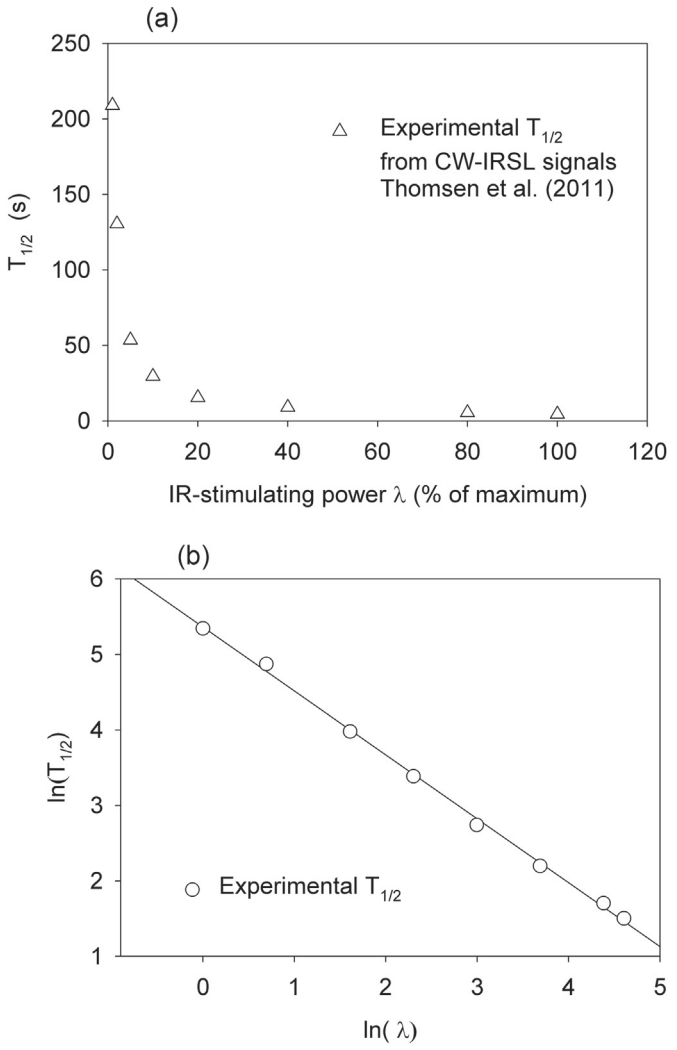

Fig. 7. (a) Half-lives of CW-IRSL signals from a K-rich extract, measured with a variable stimulating power λ (in % of maximum available stimulating power) [16] (b) the same data as in (a), plotted on a log-log scale.

cates that there are at least two sources of the CW-IRSL signals in this sample, with different stimulation cross sections. The first component is likely to be dominant at low powers, while both components are most likely making significant contributions to the CW-IRSL signal at powers above 60% of the maximum power. If the experimental data points for low powers (<60%) are fitted with a straight line, a very low value of -0.29 ± 0.02 is obtained for the slope; this large deviation from -1 is consistent with the presence of multiple components in the CW-IRSL signal from this material.

Fig. 5(a) shows a third example of applying the test in Lithium tetraborate $Li_2B_4O_7$ (LBO), a tissue-equivalent material of interest for TL dosimetry. Isothermal signals from sample LBO were measured at different temperatures in the range 135–170 °C by Kitis et al. [9]. These ITL measurements were carried out using a RISØ TL/OSL reader (model TL/OSL–DA–15), with a 9635QA photomultiplier tube and a combination of Pilkington HA-3 heat absorbing and Corning 7–59 (320–440 nm) blue filter for light detection. Fig. 5(b) shows the corresponding Arrhenius plot of $\ln(T_{1/2})$ as a function of the Arrhenius factor $1/k_BT$, yielding the activation energy $E = (0.968 \pm 0.005)$ eV. This value of E is slightly lower than the value of $E = 1.17 \pm 0.01$ eV obtained from applying several types of methods of analysis to luminescence data in this sample Kitis et al. [9].

Fig. 6(a) shows isothermal signals from a Magnesium borate (MgB_4O_7) sample (MBO), measured at different temperatures in the range 100–195 °C by Kitis et al. [9]. When an Arrhenius plot using *all* the experimental points in Fig. 6(a), the resulting graph (not shown here) is non-linear, indicating the presence of multiple traps. Fig. 6(b) shows the Arrhenius plot of $\ln(T_{1/2})$ as a function of the temperature factor $1/k_BT$, by using *only* the experimental points in the temperature subrange T = 140–195 °C. In this temperature subrange the Arrhenius plot is linear and yields the activation energy $E = (0.40 \pm 0.01)$ eV. This value of E is similar to the value $E = 0.349 \pm 0.04$ eV obtained from applying additional methods of analysis to luminescence data in this sample by Kitis et al. [9].

A final example of applying the simple test to CW-IRSL signals from feldspar is shown in Fig. 7. The sample was a K-rich sediment extract (laboratory code 951020) previously studied in Thomsen et al. [16], in Pagonis et al. [11], and in Jain and Ankjærgaard [4]. The sample was given a dose of 45 Gy and subsequently preheated to 250 °C for 60 s, prior to measurement of the IRSL signal at 50 °C using different powers of their IR LEDs. Fig. 7(a), where the CW-IRSL signals were measured with a variable stimulating power P, expressed as the percent of the maximum available IR power. The results of applying the test to this data in (a) is shown in Fig. 7(b), which results in a straight line with a slope of -0.85 ± 0.02 and a coefficient of $R^2 = 0.998$. This is an indication that the CW-IRSL signals are quite likely to originate in the same single trap, in agreement with the modeling results by Pagonis et al. [11]. The deviation of the slope from the ideal value of -1 indicates the possible presence of weak competition effects.

9. Conclusions

Table 1 summarizes all the analytical equations for the 5 models considered in this paper. In all cases the half-lives $\tau_{1/2}$ and $T_{1/2}$ are inversely proportional to the constant excitation rate λ, due to the similarities in the differential equations of the models.

It must be emphasized that the examples of experimental data given in this paper were for *prompt luminescence signals*, whose analysis yields the half-lives $T_{1/2}$.

The simple test described in this paper is a useful quick method to ascertain whether the luminescence signals in a CW-OSL, CW-IRSL or ITL experiment originate from a single trap, or from a more complex underlying luminescence process. The values of the half-lives $T_{1/2}$ can be obtained by visual inspection of the raw luminescence curves $I(t)$, and a simple log-log plot can give valuable information about the luminescence process.

Acknowledgment

We thank Dr. Kristina Thomsen for providing us with a digital copy of the experimental data shown in Fig. 7.

References

[1] R. Chen, V. Pagonis, Thermally and Optically Stimulated Luminescence: a Simulation Approach, Wiley and Sons, Chichester, 2011.
[2] R. Chen, S.W.S. McKeever, Theory of Thermoluminescence and Related Phenomena, World Scientific, 1997.
[3] C. Furetta, G. Kitis, Review models in thermoluminescence, J. Mater. Sci. 39 (2004) 2277–2294.
[4] M. Jain, C. Ankjærgaard, Towards a non-fading signal in feldspar: insight into charge transport and tunneling from time-resolved optically stimulated luminescence, Radiat. Meas. 46 (2011) 292–309.
[5] M. Jain, B. Guralnik, M.T. Andersen, Stimulated luminescence emission from localized recombination in randomly distributed defects, J. Phys. Condens. Matter 24 (2012) 385402.
[6] G. Kitis, N.D. Vlachos, General semi-analytical expressions for TL, OSL and other luminescence stimulation modes derived from the OTOR model using the Lambert W-function, Radiat. Meas. 48 (2012) 47–54.
[7] G. Kitis, V. Pagonis, New expressions for half-life, peak maximum temperature, activation energy and kinetic order of a thermoluminescence glow peak based on the Lambert W function, Radiat. Meas. 97 (2017) 28–34.

[8] G. Kitis, V. Pagonis, Analytical solutions for stimulated luminescence emission from tunneling recombination in random distributions of defects, J. Lumin. 137 (2013) 109–115.
[9] G. Kitis, G.S. Polymeris, I.K. Sfampa, M. Prokic, N. Meriç, V. Pagonis, Prompt isothermal decay of thermoluminescence in MgB4O7:Dy, Na and LiB4O7:Cu, In dosimeters, Radiat. Meas. 84 (2016) 15–25.
[10] S.L. Lovedy, R.K. Gartia, Derivation of an expression for lifetime (τ) in OTOR model, Nucl. Instrum. Meth. Phys. Res. 308 (2013a) 21–23.
[11] V. Pagonis, M. Jain, A.S. Murray, C. Ankjærgaard, R. Chen, Modeling of the shape of infrared stimulated luminescence signals in feldspars, Radiat. Meas. 47 (9) (2012) 870–876.
[12] V. Pagonis, G. Polymeris, G. Kitis, On the effect of optical and isothermal treatments on luminescence signals from feldspars, Radiat. Meas. 82 (2015) 93–101.
[13] G.S. Polymeris, E. Theodosoglou, G. Kitis, N.C. Tsirliganis, A. Koroneos, K.M. Paraskevopoulos, Mediter. Archaeol. Archaeom. 13 (2013) 155–161.
[14] G.S. Polymeris, OSL at elevated temperatures: towards the simultaneous thermal and optical stimulation, Radiat. Phys. Chem. 106 (2015) (2015) 184–192.
[15] Singh L. Lovedy, R.K. Gartia, Derivation of a simplified OSL OTOR equation using Wright Omega function and its application, Nucl. Instrum. Meth. Phys. Res. B 346 (2015) 45–52.
[16] K.J. Thomsen, A.S. Murray, M. Jain, Stability of IRSL signals from sedimentary K-feldspar samples, Geochronometria 38 (2011) 1–13.